

Short Communication

## Poly(methyl methacrylate-co-N-vinyl-2-pyrrolidone polymer as inhibitor for Mild Steel Corrosion in Acidic Media

Xiqing Zhao<sup>1,\*</sup>, Jun Xiong<sup>2</sup>, Shaowei Zhu<sup>3</sup>, Xiaosong Zhao<sup>3</sup>, Ambrish Singh<sup>4</sup>

<sup>1</sup> Qiqihar Medical University, Qiqihar, Heilongjiang Province, 161006, P.R China

<sup>2</sup> No.5 Testing Institute of Beijing Construction Quality Co., Ltd., Beijing, 100000, P.R. China

<sup>3</sup> Qiqihar University, Heilongjiang Province, 161006, China

<sup>4</sup> School of Materials Science and Engineering, Southwest Petroleum University, 8 Xindu district-610500, Chengdu city, Sichuan province, P.R. China.

\*E-mail: [zhaoxiqingssl@sina.com](mailto:zhaoxiqingssl@sina.com)

Received: 9 September 2018 / Accepted: 25 October 2018 / Published: 30 November 2018

---

A thorough investigation of a polymer was performed for corrosion of mild steel in 1M HCl solution using electrochemical and surface studies. Infra-red spectroscopy was completed in reflectance mode to detect the adsorption of the polymer on the metal surface. Scanning electrochemical microscopy (SECM) studies were made to detect the localized corrosion reaction at the working electrode. Electrochemical impedance spectroscopy revealed that the efficiency of corrosion inhibition was improved after the addition of polymer in the solution. Polarization studies suggested that the polymer belong to the mixed category mitigators. Scanning electrochemical microscopy (SECM) studies suggested that the surface was insulating in presence of polymer thereby protecting the surface. Scanning electron microscope (SEM) suggested that the surface was less corroded in presence of polymer.

---

**Keywords:** SECM, Polymer, SEM, FTIR, Mild steel, EIS

### 1. INTRODUCTION

Deterioration of metals is an environmental process involving electrochemical reactions in presence of water and oxygen. There are many available methods to mitigate corrosion of metals from corrosive environment. Addition of compounds to the reacting environment that can reduce the rate of corrosion is known as inhibition method and the compounds are called inhibitors or mitigators. There are several kinds of inhibitors available. The strict regulations of toxicity control do not allow the use of synthetic/organic inhibitors in large amounts [1]. So, the development of inhibitors based on green

principles is always in demand. These are widely used in industries as they are cheap and easy to apply. The inhibitors usually adsorb on the metal surface forming a protective film that prevents the corrosive media to interact with the metal surface. The inhibitor molecules are rich in atoms and functional groups that can form complex and bonds with the vacant orbital of the metals. The intact film of inhibitor on the surface can keep the metal safe for a long period of time till the film is washed away or a crack/scratch appears on the surface [2-6].

The use of polymers as inhibitor for metal corrosion is globally preferred as they have repeating units of monomers which can cover the entire metal surface. The active centers responsible for anodic activity can be suppressed by these monomers covering the wide regions. Along with these abilities polymers are very stable and cost effective [7]. The complex formed between the metal and polymer is very strong and can retain for long time. Most of the polymers are known to perform well at higher temperature which makes them suitable to use in transport pipelines passing through deserts or in oil well with high temperature and high pressure. Synthetic and natural polymers have been studied extensively as inhibitors for different corrosive mediums [8]. One of the major concerns related with polymers is their insoluble nature. To increase the solubility several methods such as functionalization and copolymerization have been adopted. The polymers that are easily soluble have varied applications in corrosion and scale related situations.

This paper includes the study of one water soluble polymer prepared through copolymerization using two different monomers. After synthesis, characterization was done to verify the purity of the prepared polymer. Further, the electrochemical and surface studies were carried out at the optimum concentration of the poly(methyl methacrylate-co-N-vinyl-2-pyrrolidone) polymer hereby referred as P(MMA-co-VP).

## 2. EXPERIMENTAL

### 2.1. Synthesis of Polymer

Two monomers 2-(methoxycarbonyl)-1-propene (MMA) monomer and N-vinyl-2-pyrrolidone (NVP) monomer were dissolved in water in equivalent ratio. Potassium peroxydisulfate (KPS) was added to the solution as an initiator with continuous stirring at 75°C. The process was kept running till a white emulsion was obtained after four hours. The poly(methyl methacrylate-co-N-vinyl-2-pyrrolidone) polymer hereby referred as P(MMA-co-VP) was filtered, and dried using vacuum rotator. Different concentration of solutions was prepared refluxing with 1M HCl which were further used for the electrochemical and surface studies. The structure of the synthesized polymer is given in Figure 1.

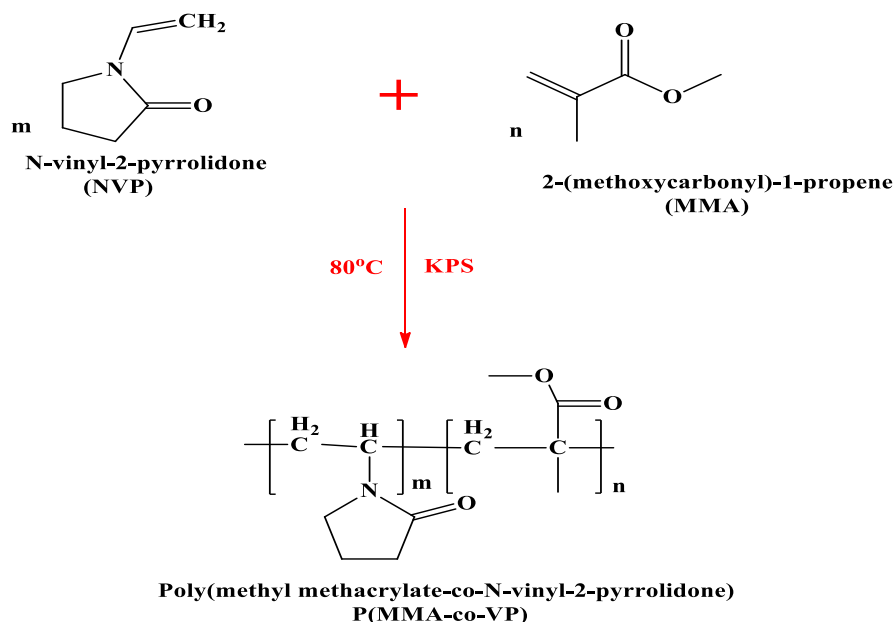


**Figure 1.** Synthesis scheme of P(MMA-co-VP) polymer.

## 2.2. Materials and Solutions

All the tests were performed on metallographically abraded mild steel according to ASTM A262 standard. The mild steel samples were abraded using sand papers of different grades to give the samples a reflecting finish. The samples were washed repeatedly with water and alcohol to remove any kind of contamination and then dried at room temperature. The specimens were covered with epoxy resin and a  $1\text{ cm}^2$  area was used for the electrochemical studies. The corrosive solution of 1M HCl was prepared by using high strength and pure hydrochloric acid solution with pure refined water.

## 2.3. Fourier Transform Infrared Spectroscopy (FTIR)

Infra-red was carried out in reflectance mode using NICOLET 6700 equipped with OMNIC software. The synthesized polymer was used to carry out all the experiments and the metal samples were presented under the spectrophotometer. The reflectance mode can detect the adsorption onto the metal surface by the inhibitor.

## 2.4. X-Ray Diffraction (XRD)

The dried powder of the polymer was examined using X-RAY diffractometer. The powder was

further analyzed by Higscore software to see and verify the peaks.

## 2.5. Nuclear Magnetic Resonance (NMR) Spectroscopy

In order to verify the purity of the synthesized polymer NMR tests were conducted. This would clarify the absence of contaminants and peaks of the synthesized polymer.  $^{13}\text{C}$  and  $^1\text{H}$  NMR was conducted using Bruker instrument to study the interaction of molecules involving the test solutions.

## 2.6. Electrochemical measurements

All the electrochemical experiments were conducted using Autolab workstation. The working electrode (mild steel), reference electrode (saturated calomel electrode), and auxiliary electrode (platinum) were assembled together in a cell to carry out the reactions at room temperature. The results obtained through experiments were analyzed using FRC software. Before the start of each test an immersion time of 30 minutes was allowed in order to achieve a stable corrosion potential. Impedance experiments were performed in a frequency range from 100 kHz to 0.00001 kHz through amplitude of 10 mV. Usually small amplitude ( $\sim 10$  mV) overlaid on the dc potential can be completely portrayed by the impedance that provides the linear function of the applied perturbation.

Potentiodynamic polarization tests were conducted at a scan rate of  $1 \text{ mV s}^{-1}$  and by varying the potential from  $-300$  to  $+300$  mV vs. SCE. The anodic and cathodic plots of the polarization curves were examined to get different parameters. The efficiency of corrosion inhibition was calculated using the following relation

$$\eta\% = \frac{I_{\text{corr}}^{\text{B}} - I_{\text{corr}}^{\text{I}}}{I_{\text{corr}}^{\text{B}}} \times 100 \quad (1)$$

where,  $I_{\text{corr}}^{\text{B}}$  and  $I_{\text{corr}}^{\text{I}}$  are the corrosion current density in lack and in presence of polymer. The efficiency of polymer as inhibitor was calculated using the charge transfer resistance values as under:

$$\eta\% = \frac{R_{\text{ct}}^{\text{I}} - R_{\text{ct}}^{\text{B}}}{R_{\text{ct}}^{\text{I}}} \times 100 \quad (2)$$

where,  $R_{\text{ct}}^{\text{I}}$  and  $R_{\text{ct}}^{\text{B}}$  are the charge transfer resistance in presence and in absence of inhibitor, respectively.

## 2.7. Surface Morphological Studies

### 2.7.1. Scanning Electron Microscopy (SEM)

The mild steel samples after the electrochemical tests were washed with acetone to remove the corrosion products and then dried at room temperature. The steel samples were exposed to Zeiss Tescan instrument to get the high resolution images of the surface. Gold spray was also done to get better conductivity and high quality images as the metal samples were small in size.

### 2.7.2. Scanning Electrochemical Microscopy (SECM)

Micro-electrochemical techniques are a boon nowadays to study the corrosion reaction at the metal surface locally and point to point. The set up needs careful handling and the results obtained are very relevant and supportive to the research work [9]. The varied modes can be very informative and can provide extra mileage to the work done. The specific mild steel samples were used for the study using CHI900C instrument. A 10  $\mu\text{m}$  platinum tip is used as a probe to conduct the micro-electrochemical experiments in a cell assembly similar to electrochemical tests [10].

## 3. RESULTS AND DISCUSSION

### 3.1. Fourier transform infra-red spectroscopy

The peaks obtained as in Figure 2 are  $766.78\text{ cm}^{-1}$ ;  $855.23\text{ cm}^{-1}$ ;  $942.23\text{ cm}^{-1}$  -OH group/ olefin's single substitution;  $1021.29\text{ cm}^{-1}$  C-O bending;  $1076.67\text{ cm}^{-1}$  C-O stretching;  $1151.94\text{ cm}^{-1}$  C-H bending;  $1207.55\text{ cm}^{-1}$  C=C (Aromatic)/ C-O stretching;  $1249.56\text{ cm}^{-1}$  C=C stretching;  $1409.03\text{ cm}^{-1}$  C-H bending;  $1536.33\text{ cm}^{-1}$  N-H stretching;  $1645.77\text{ cm}^{-1}$  C=C stretching;  $1744.83\text{ cm}^{-1}$  C-O stretching;  $2829.72\text{ cm}^{-1}$  C = O (antisymmetric stretching vibration);

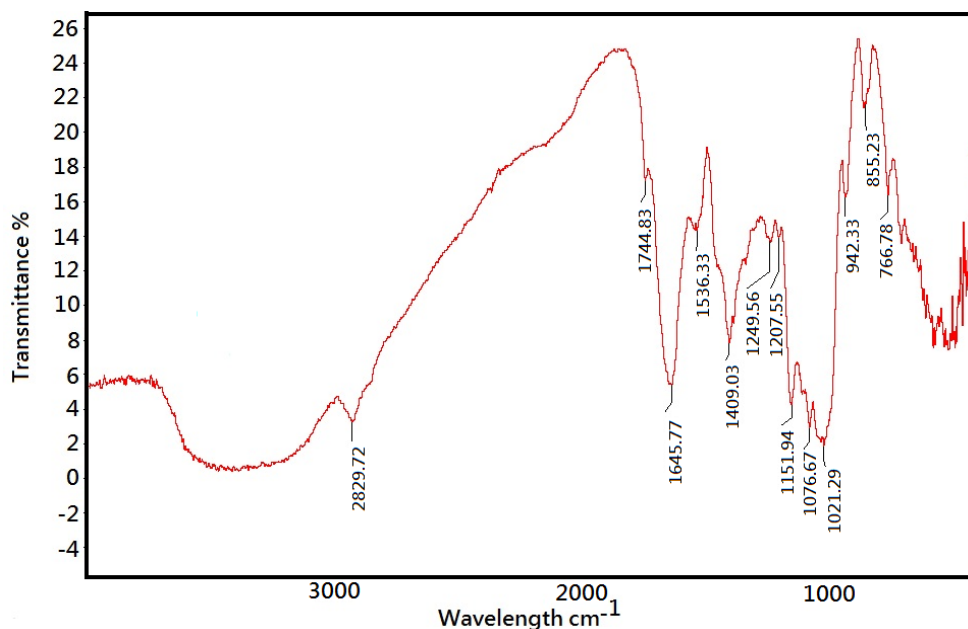


**Figure 2.** FTIR analysis of P(MMA-co-VP) polymer.

### 3.2. X-Ray Diffraction (XRD)

Diffraction study was made using X-Ray machine X-pert pro. The peaks of the polymer with respect to immersion time were recorded as shown in Figure 3. The peaks appeared at the lower values that are known to be more specific. The peaks were broad in nature even though the lower  $2\theta$  degrees

were due to the lack of recrystallization nature of the polymer used in the method.

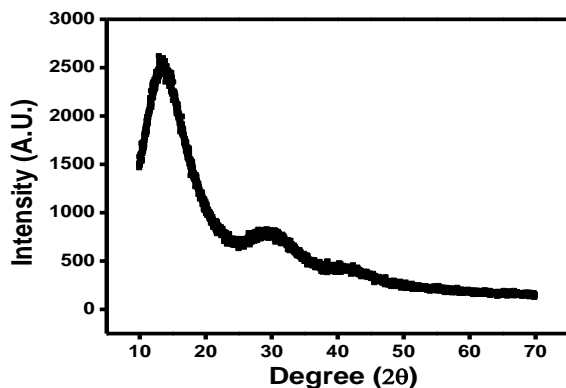
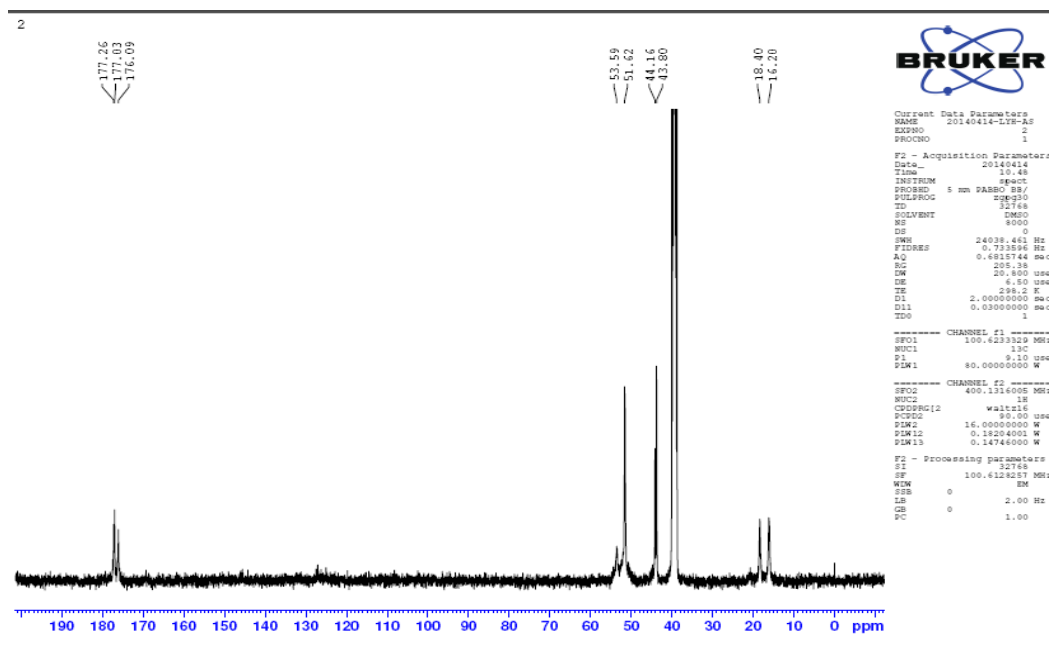


Figure 3. XRD analysis of P(MMA-co-VP) polymer.

### 3.3. Nuclear Magnetic Resonance (NMR) Spectroscopy

<sup>1</sup>H NMR peaks in Figure 4a are as follows: CH<sub>3</sub> (methylmethacrylate) 0.742 to 1.454 ppm; <sup>4</sup>CH<sub>2</sub> 2.948 ppm; <sup>2</sup>CH<sub>2</sub> 1.812 ppm; <sup>3</sup>CH<sub>2</sub> 1.756 ppm; OCH<sub>3</sub> 3.557 ppm.

<sup>13</sup>C NMR peaks obtained as in Figure 4b are as follows: <sup>4</sup>CH<sub>2</sub> 43.80 ppm; CH<sub>2</sub> 18.40 ppm; CH<sub>3</sub> (methylmethacrylate) 16.20 ppm; CH (vinyl) 44.16 ppm; OCH<sub>3</sub> (methylmethacrylate) 51.62 ppm; CH<sub>2</sub> (methylmethacrylate and vinyl) 53.59 ppm.



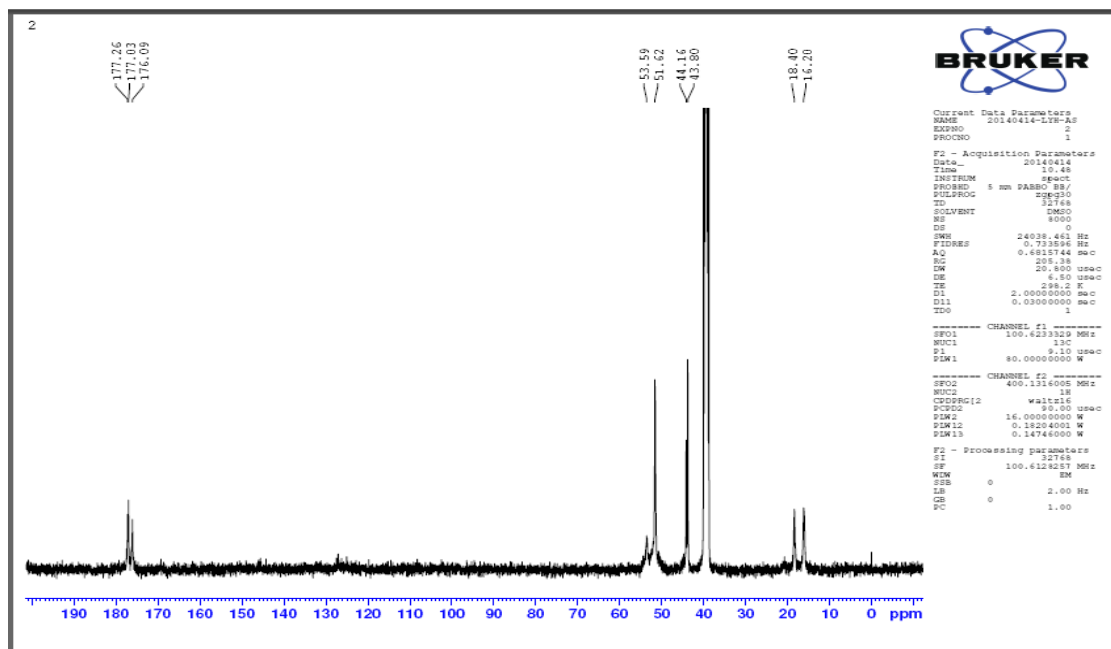


Figure 4. NMR study of <sup>1</sup>H and <sup>13</sup>C of P(MMA-co-VP) polymer.

### 3.4. Electrochemical measurements

#### 3.4.1. Potentiodynamic polarization measurements

The potentiodynamic polarization curves of the mild steel in corrosive media with and without polymer are shown in Figure 5. The shift in both anodic and cathodic regions suggested that the corrosion reaction was directed by the transfer of electrons at the electrode surface. Table 1 shows the corrosion potential ( $E_{corr}$ ), corrosion current density ( $I_{corr}$ ), and anodic ( $\beta_a$ ) and cathodic ( $\beta_c$ ) slopes evaluated after the polarization tests [11, 12].

The corrosion current density values in Table 1 indicated that the addition of polymer to the corrosive system decreases the rate of corrosion. This can be attributed to the complex formed between the polymer and the metal that blocks the corrosive media to interact with the electrode surface [13]. The polarization curves for mild steel with and without polymer are given in Figure 5.

Table 1. Polarization data for mild steel in 1M HCl for various concentrations of P(MMA-co-VP) at 298 K.

Solution	Polarization data					
	$E_{corr}$ (V vs. SCE)	$I_{corr}$ ( $\mu\text{A cm}^{-2}$ )	$b_a$ ( $\text{mV d}^{-1}$ )	$b_c$ ( $\text{mV d}^{-1}$ )	$\eta$ (%)	$\theta$
Without P(MMA-co-VP)-	-0.510	67	98	65	-	
P(MMA-co-VP) 50 ppm	-0.539	12	62	76	82	0.82
100 ppm	-0.523	7	48	57	90	0.90
200 ppm	-0.527	4	33	42	94	0.94

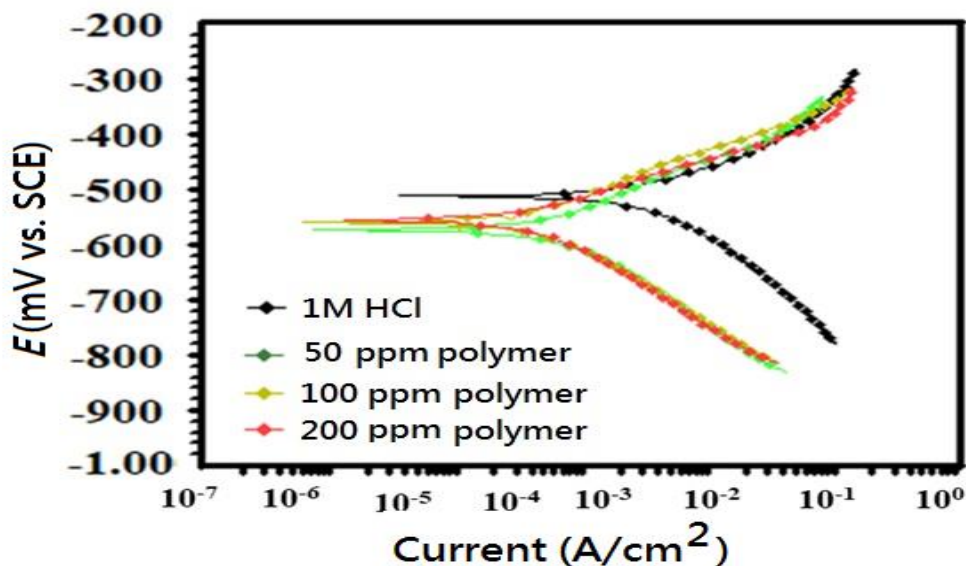


**Figure 5.** Polarization plots for mild steel in 1M HCl with and without P(MMA-co-VP).

### 3.4.2. Electrochemical Impedance Spectroscopy

Impedance studies were carried out to investigate about the redox reaction taking place at the metal surface. The oxidation of mild steel due to presence of the corrosive HCl solution and evaluation of hydrogen provides the description of the reaction taking place at the electrode due to its electrochemical reaction [14, 15]. The transfer of electrons was controlled kinetically as the obtained semicircles of the Nyquist curves are similar in shape as shown in Figure 6 [16, 17]. The high frequency capacitive loop can be observed from the figure that also corresponds to the circuit used to fit the impedance data. The diameter of the capacitive loop becomes bigger with the addition and increase in polymer concentration. This could be attributed to the roughness at the surface, random active centers, or adsorption of the diverse P(MMA-co-VP) molecules [18].

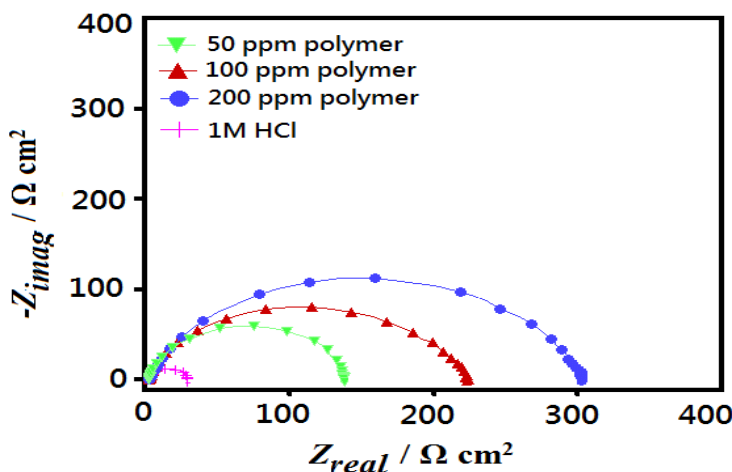


**Figure 6.** Nyquist plots for mild steel in 1M HCl without and with P(MMA-co-VP) .

**Table 2.** Nyquist data for mild steel in 1M HCl for various concentrations of P(MMA-co-VP).

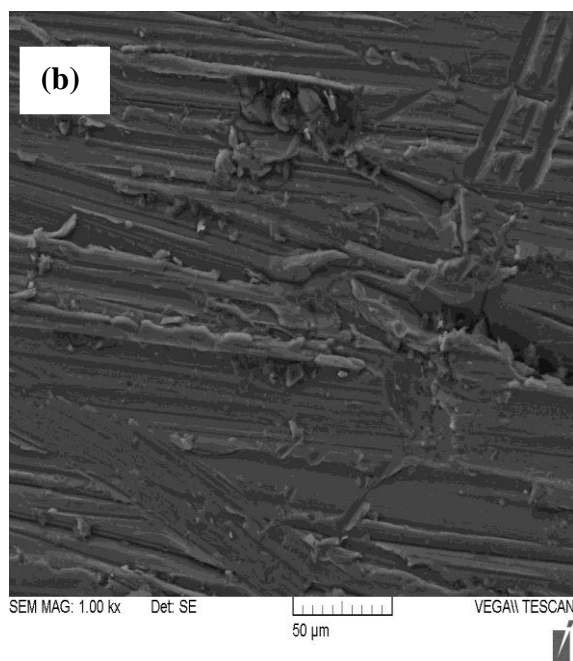
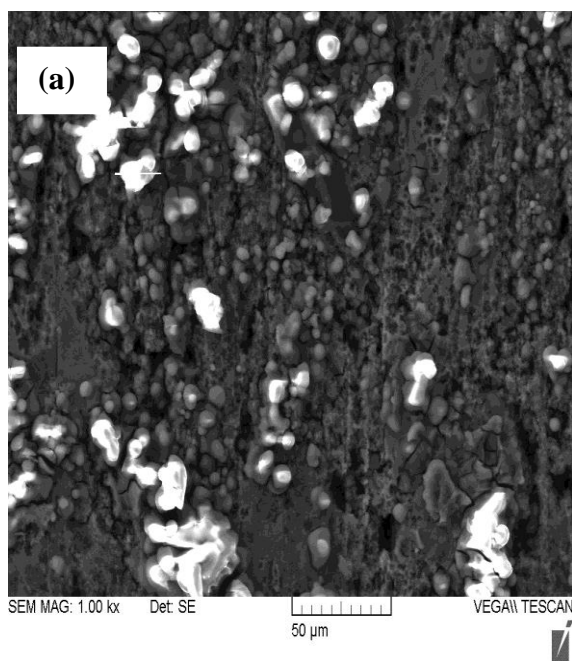
Solutions (ppm)	$R_{ct}$ ( $\Omega\text{ cm}^2$ )	$n$	$Y^{-1}$ ( $\Omega^{-1}\text{s}^n/\text{cm}^2$ )	$\eta$ %	Surf. coverage $\theta$
Without P(MMA-co-VP)	15	0.77	0.31	-	-
50 ppm	135	0.79	0.26	89	0.89
100 ppm	215	0.83	0.29	93	0.93
200 ppm	303	0.86	0.19	97	0.95

The efficiency of the polymer for corrosion of mild steel was found to increase with increase in the concentration. The increase in charge transfer resistance values as shown in Table 2 is due to the film formed by the polymer on the surface that increases the resistance to corrosion reaction [19, 20].

### 3.5. Surface Analyses

#### 3.5.1. Scanning Electron Microscopy (SEM)

The mild steel samples used in electrochemical experiments were washed with sodium bicarbonate solution followed by acetone to remove the contaminants and the corrosion products. The samples were then dried at room temperature and kept in desiccator [21]. The samples were then taken to the Zeiss Tescan instrument to conduct the tests of the surface to get high resolution micrographs through SEM. The samples were also sprayed with gold for better conductivity of the surface and to get high quality figures. Figure 7a shows the surface of the metal sample that is very corroded and rough in absence of the polymer. While in the presence of the polymer the surface of mild steel is quite smooth and uniform as shown in Figure 7b, 7c and Figure 7d. So, the surface of mild steel was less corroded in presence of polymer and rough in its absence [22, 23].



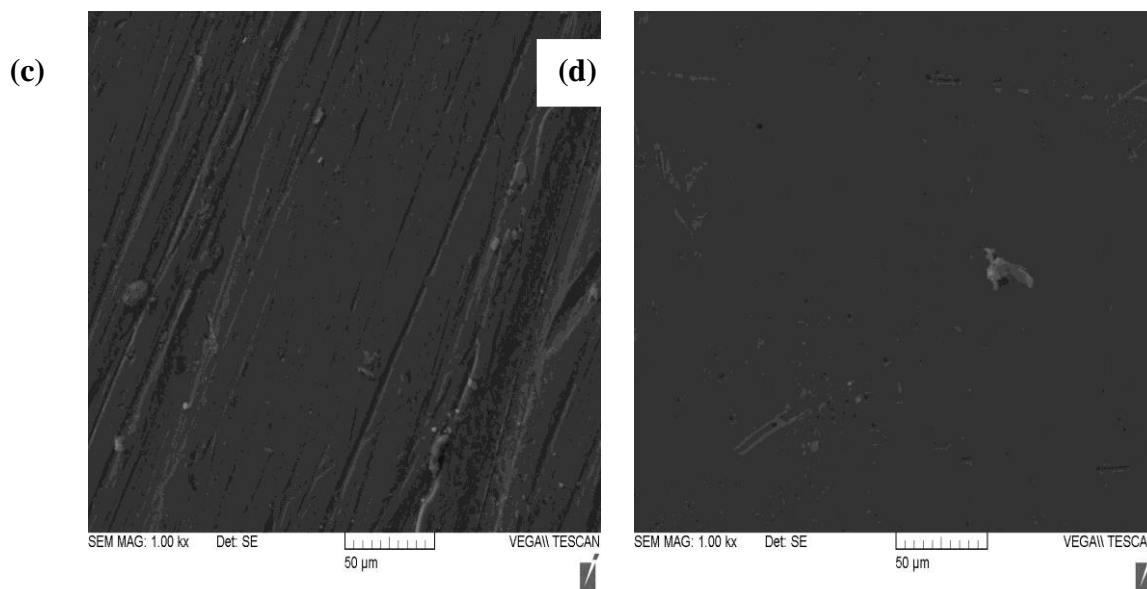


**Figure 7.** SEM images for (a) 1M HCl solution (b) 50 ppm P(MMA-co-VP) (c) 100 ppm P(MMA-co-VP) and (d) 200 ppm P(MMA-co-VP) .

3.5.2. Scanning Electrochemical Microscopy (SECM)

The micro-electrochemical techniques have proved their existence while being informative and resourceful for its operation on insulating and conducting metal surfaces [24, 25]. These techniques can be used in variant modes to study the localized corrosion. The mild steel samples were cut in specified dimensions to fit in the CHI instrument to carry out the SECM experiments.

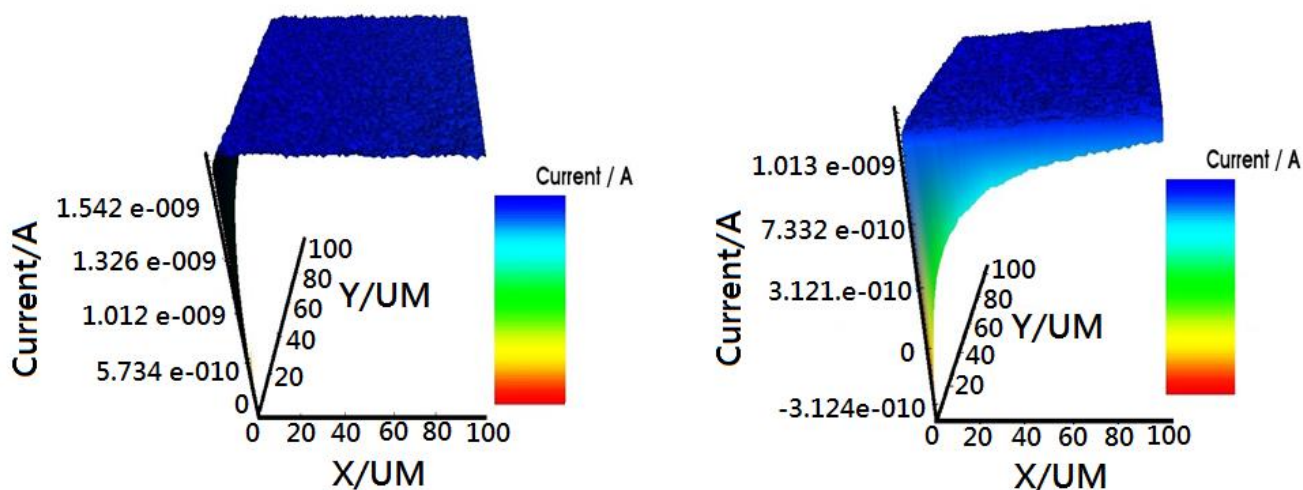


**Figure 8.** SECM 3D images for 1M HCl and 1000 ppm P(MMA-co-VP)

The cell was assembled with three electrode system and a platinum probe was used to vibrate over the metal surface to receive the information on corrosion reactions. The probe was established at an equi-distance over the mild steel surface using the probe approach curve mode before the start of each

test [26, 27]. Figure 8a, b shows the 3D picture of the scan done through SECM mode by the instrument. The mild steel surface was observed to act as conductor in absence of the polymer as this is evident from the figure where the current was higher as the steel was in direct contact with the probe. While, when the metal surface intact with polymer film was exposed to the vibrating probe, the current observed was lower due to the non contact between metal surface and the probe. This observation was due to the insulating action of the metal covered with polymer film. After comparing the currents of metal surface with and without polymer film the protective action of the inhibitor could be verified [28-33].

#### 4. CONCLUSIONS

- The present study showed the protective action of P(MMA-co-VP) polymer on mild steel surface in 1M HCl solution through electrochemical and surface studies.
- The impedance studies revealed that the charge transfer resistance was found to increase along with the diameter of Nyquist plots with increase in the polymer concentration.
- The polarization techniques showed the decrease in corrosion current density values with increase in polymer concentration. This led to the better corrosion efficiency shown by the polymer. The anodic and cathodic shift in the corrosion potential showed that the polymer belong to the mixed category.
- SEM images with smooth surface confirmed the inhibition action of the polymer on the mild steel. SECM technique also suggested the insulating action of the polymer film on the electrode surface.

#### ACKNOWLEDGEMENTS

Authors are thankful to the financial assistance from the science and technology plan project of Qiqihar, China (GYGG-201702).

#### References

1. Ambrish Singh, K.R. Ansari, Jiyaul Haque, Parul Dohare, Hassane Lgaz, Rachid Salghi, M.A. Quraishi, *J. Taiwan Inst. Chem. E.*, 82 (2018) 233.
2. A. Singh, K. R. Ansari, X. Xu, Z. Sun, A. Kumar, Y.Lin, *Sci. Report.*, 7 (2017) 14904
3. G. Gece, *Corros. Sci.*, 53 (2011) 3873.
4. I. Ahamad, R. Prasad, M.A. Quraishi, *Corros. Sci.*, 52 (2010) 3041.
5. K. F. Khaled, M. A. Amin, *Corros. Sci.*, 51 (2009) 1964-1975.
6. A. Singh, K.R. Ansari, J. Haque, P. Dohare, H. Lgaz, R. Salghi, M.A.Quraishi, *J. Taiwan Inst. Chem. E.*, 82 (2018) 233.
7. D. K. Yadav, D. S. Chauhan, I. Ahamad, M. A. Quraishi, *RSC. Adv.* 3 (2013) 632.
8. A. Singh, E. E. Ebenso, M. A. Quraishi, Y. Lin, *Int. J. Electrochem. Sci.*, 9 (2014) 7495.
9. B. M. Quinn, I. Prieto, S. K. Haram, A. J. Bard, *J. Phys. Chem. B.*, 105 (2001) 7474.
10. A. J. Bard, G. Denuault, C. Lee, D. Mandler, D. O. Wipf, *Acc. Chem. Res.*, 23 (1990) 357-363.
11. Hongwei Feng, Ambrish Singh, Yuanpeng Wu, Yuanhua Lin, *New. J. Chem.*, (2018) DOI: 10.1039/c8nj01676c.

12. Songsong Chen, A. Singh, Yuanluqi Wang, Wanying Liu, Kuanhai Deng, Yuanhua Lin, *Int. J. Electrochem. Sci.*, 12 (2017) 782.
13. Hongqiang Wan, Peiying Han, Shuai Ge, Fancong Li, Simiao Zhang, Huan Li, A. Singh, *Int. J. Electrochem. Sci.*, 13 (2018) 9302.
14. Haolong Yang, Ming Zhang, A. Singh, *Int. J. Electrochem. Sci.*, 13 (2018) 9131-9144.
15. M. A. Quraishi, A. Singh, V. K. Singh, D. K. Yadav, A. K. Singh, *Mater. Chem. Phys.*, 122 (2010) 114.
16. A. Singh, K. R. Ansari, M. A. Quraishi, Hassane Lgaz and Yuanhua Lin, *J. Alloys Comp.*, 762 (2018) 347.
17. X. Li, S. Deng, H. Fu, *Corros. Sci.*, 53 (2011) 3241.
18. A. Singh, I. Ahamad, M. A. Quraishi, *Arab. J. Chem.*, 9 (2016) S1584.
19. D. K. Yadav, M. A. Quraishi, B. Maiti, *Corros. Sci.*, 55 (2012) 254.
20. A. Singh, I. Ahamad, V. K. Singh, M. A. Quraishi, *J. Solid State Electrochem.*, 15 (2011) 1087.
21. Zhipeng Sun, Ambrish Singh, Xihua Xu, Songsong Chen, Wanying Liu, Yuanhua Lin, *Res. Chem. Inter.*, 43 (2017) 6719.
22. Xihua Xu, A. Singh, Z. Sun, K. R. Ansari, Y. Lin, *R. Soc. Open Sci.*, 4 (2017) 170933.
23. Priyanka Singh, Ambrish Singh, M.A. Quraishi, *J. Taiwan Inst. Chem. E.*, 60 (2016) 588.
24. A. Singh, Y. Lin, Chunyang Zhu, Y. Wu, E. E. Ebenso, *Chin. J. Pol. Sci.*, 33 (2015) 339.
25. Chitrasen Gupta, Ishtiaque Ahamad, A. Singh, Xihua Xu, Zhipeng Sun, Yuanhua Lin, *Int. J. Electrochem. Sci.*, 12 (2017) 6379.
26. Ambrish Singh, Y. Lin, W. Liu, S. Yu, J. Pan, C. Ren, D. Kuanhai, *J. Ind. Eng. Chem.*, 20 (2014) 4276.
27. A. Singh, Yuanhua Lin, K. R. Ansari, M. A. Quraishi, E. E. Ebenso, Songsong Chen, W. Liu, *Appl. Surf. Sci.*, 359 (2015) 331.
28. A. Singh, Y. Lin, W. Liu, E. E. Ebenso, J. Pan, *Int. J. Electrochem. Sci.*, 8 (2013) 12884.
29. Ambrish Singh, Y. Lin, I. B. Obot, E. E. Ebenso, K. R. Ansari, M. A. Quraishi, *Appl. Surf. Sci.*, 356 (2015) 341.
30. A. Singh, Y. Lin, I. B. Obot, E. E. Ebenso, *J. Mol. Liq.*, 219 (2016) 865.
31. A. Singh, K. R. Ansari, M. A. Quraishi, Hassane Lgaz, Yuanhua Lin, *J. Alloys Comp.*, 762 (2018) 347.
32. X. Li, S. Deng, H. Fu, *Corros. Sci.*, 53 (2011) 3241.
33. Yuanhua Lin, Ambrish Singh, E. E. Ebenso, Yuanpeng Wu, Chunyang Zhu, H. Zhu, *J. Tai. Inst. Chem. Eng.*, 46 (2015) 214.